MECHANICAL PROPERTIES OF MATRIX HYBRID COMPOSITES WITH MECHANICAL JOINT

Kenichi Sugimoto, Akihiro Ochi, Asami Nakai, Hiroyuki Hamada*

Abstract

In this paper, the effect of stacking sequence and laminate thickness on mechanical behavior of matrix hybrid composite with mechanical joint was investigated to improve the performance of composite structures for automotives. Four types of stacking sequences of matrix hybrid and two kinds of laminate thickness were prepared. The failure maximum load depended on the characteristic of matrix resin and laminate thickness. The optimum stacking sequence, especially in case of thick laminate, was expected by placing conventional resin, that is rigid resin into outer domain and flexible resin into inner domain.

Background

Recently, the automotive industry is greatly concerned with global warming which caused by the exhaust, so that the lightweight is necessary. Therefore use of FRP (Fiber Reinforce Plastic) in the automotives instead of steel has to be promoted. Generally, the most of structures should possess the joint part, and mechanical joint is often used among the several joint methods. In case of mechanical joint, the hole has to be made in order to fasten by using bolt and rivet, so that the strength of joint part decreases due to the stress concentration. The fracture aspects of mechanical joint are Net-Tension, Bearing, Shear-Out failure and so on. In case of a small width, Net-Tension failure often occurs. Shear-Out failure occurs when end distance is small. The joint with the large width and large end distance fails in Bearing failure which shows ductile manner and the higher failure load than in Net-tension and Shear-out. Therefore, the design of mechanical joint failed in Bearing is demanded.

In this study, the effect of stacking sequence on mechanical behavior of matrix hybrid composite with mechanical joint was examined. Matrix hybrid composite is that two or more matrix resins are combined in a laminates in order to improve the performance of composite laminates. And fracture aspects based on precise cross-sectional observation of fracture zone were discussed.

Material

The 0º/90º multi-axial warp knitted fabric was used as reinforcement. The schematic diagram of 0º/90º multi-axial warp knitted fabric is shown in Figure 1. Multi-axial warp knitted fabric allows the placement of warp, weft, and off-axis materials directly into the fabric structure. The composites with the multi-axial warp knitted fabric can possess higher mechanical properties, because of no crimp of reinforcement. Moreover, not only the unidirectional fiber bundles, but also chopped strand mat can be combined. Multi-axial warp knitted fabric has the ability to combine multiple layers of oriented yarn in a single structure. This reduces the cost with omission of the stacking process.

Two kinds of unsaturated polyester resins were used as matrix. One is conventional resin used for general purpose and the other is flexible resin as summarized in Table I. The modulus and strength of flexible resin are lower than those of conventional resin, however, the fracture toughness of flexible resin is much higher. In following section, the conventional resin is called as rigid resin.

Experimental Method

Four types of stacking sequences for matrix hybrid composite laminates were used as shown in Figure 2. (a) and (b) consisted of only rigid resin(Type R) and only flexible resin(Type F) respectively. In Figure 2(c), rigid resin was placed at outer layer and flexible resin was placed at inner layer (Type RFR). The stacking sequence in Figure 2(d) was the reverse of that in Figure 2(c)(Type FRF).

Two kinds of laminate thickness were prepared by changing the number of ply. One was thin laminate in 2.8mm with 4 plies and the other was thick laminate in 11.0mm with 16 plies. All specimens were fabricated by hand-lay-up technique in symmetrical stacking sequence as shown in Figure 2 (i.e. thin was $[0º/90º]_{2s}$ and thick was $[0º/90º]_{8s}$).

The specimen geometry is shown in Figure 3. The length, width and hole diameter of specimen were 200mm, 30mm and 10mm, respectively. The center of hole was at center in width direction and 30mm distance from edge of specimen. Joint tests were performed by using INSTRON testing machine (type 4206) at a constant cross-head speed of 1.0mm/min.

Results and Discussions

Joint test

Typical load-displacement curves obtained from joint test of the thin specimen are shown in Figure 4(a). In R, RFR and FRF specimen, the load increased almost

linearly and decreased drastically after maximum point. Regarding F specimen, the load kept in almost constant value after maximum.

Figure 4(b) shows typical load-displacement curves obtained from joint test of the thick specimen. Regarding all stacking sequence, the load was increased almost linearly until the maximum load and then decreased. The dependence of consisting resin on load-displacement stiffness appeared in thick specimen. In the case of R and RFR specimen, the decrease in load after maximum point was smaller compared with each of thin specimens.

The experimental results of joint test are shown in Table II. The maximum load of R specimen was the highest and that of F specimen was the lowest in both thicknesses. The maximum loads of RFR and FRF specimen were similar values. Also, the ratio of each maximum load to the maximum load of R specimen; P/P_R, and the value of maximum load divided by laminate thickness; P/t were listed in Table II. Both P/P_R and P/t for thick specimens were higher than those for thin specimens. The value of P/t of R, F, RFR and FRF specimens changed from 2.66 to 3.44, 1.73-2.65, 2.33-2.91 and 2.25-3.21 respectively. From these results, the degree of increase in P/t of FRF specimen was higher than any other specimens.

Observation of cross section

Observation of failure part (See Figure 5) was performed. The optical microscopic observation of thin specimen is shown in Figure 6. In R specimen, the out-plane deformation occurred as shown in Figure 6(a). The delamination between 0º/90º interlamina at outermost layers was developed along the longitudinal direction. Figure 6(b) indicates the fracture aspect of F specimen. It was observed that the local large out-plane deformation of outermost layers and slant cracks resulting from shear fracture were generated.

The fracture aspect of RFR specimen is shown in Figure 6(c). The out-plane deformation and large delamination were observed. These cracks of delamination were generated between 0º/90º interlamina at the outer domain with rigid layer and also between rigid and flexible layer. Regarding FRF specimen, only a large crack at the middle layer consisted of rigid resin was observed as shown in Figure 6(d). Over all thin specimen, it was observed that shear fracture occurred from outer layer to inner layer.

The failure aspects of thick specimens are shown in Figure 7. Over all, slant cracks caused by shear fracture were generated from inner layer in thickness direction outwards. This was opposite to the failure pattern of thin specimens. On the final failure aspect, delamination at rigid layer and large slant cracks resulting from shear fracture at flexible layer were dominant as same as thin specimen. However regarding R specimen, delamination was observed at only outer layer as shown in Figure 7(a). Similarly, delamination at rigid inner layer was seen in FRF specimen as shown in Figure 7(d).

The characteristic of matrix resin clearly affected failure aspects. Delamination was governed at rigid layer with low fracture toughness. On the contrary, flexible layer with high fracture toughness restrained delamination, however, tended to fail in shear. The fracture aspects of thin specimen were mainly delamination or local shear fracture. On the other hand, those of thick specimen were mainly large slant cracks due to shear fracture. Furthermore the fracture aspects of inner and outer layer were different for thick specimen. From these results, it was expected that the local out-plane deformation caused pin-loading depended on laminate thickness which relating to local bending deformation. Thin specimen was easily deformed in out-plane, so that no difference in fracture aspects of inner and outer layer was observed. On the other hand, in case of thick specimen, the out-plane deformation occurred at only outer layer, so that inner layer without out-plane deformation was directly loaded in compression longitudinally. As a result, slant cracks due to shear fracture generated from middle layer to outer layer.

Accordingly thin specimen was deformed easily in out-plane, so that the bending stiffness affected remarkably whole mechanical behavior. On the contrary, the only outer layer was deformed in out-plane for thick composite. Consequently the stacking sequence of FRF specimen is possible that higher maximum load can be obtained because the outer domain with flexible layer restrain delamination in out-plane deformation and rigid layer was placed at inner domain with higher compression property.

As a future work, more precise observation is required to clarify the above discussion. Moreover, the optimum stacking sequence for increase in failure load will be investigated.

Conclusion

In this study, the effect of stacking sequence and laminate thickness on mechanical behavior of matrix hybrid composite with mechanical joint was examined. The maximum load depended on characteristic of matrix resin and increased with increase in laminate thickness. The fracture aspect was changed remarkably by stacking sequence of matrix hybrid and laminate thickness.

Tables & Figures

Table I: Mechanical properties of matrix resin.

	Modulus, E (GPa)	Strength, σ (MPa)	Fracture Toughness K_c (MPa $m^{1/2}$)
Conventinal resin	3.29	108.60	0.31
Flexible resin	2.23	81.30	0.79

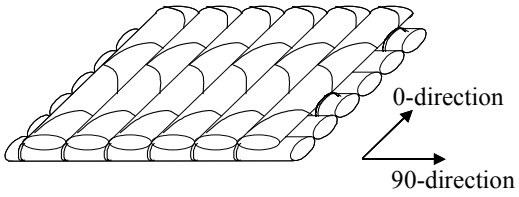

Figure 1: 0°/90° multi-axial warp knitted fabric.

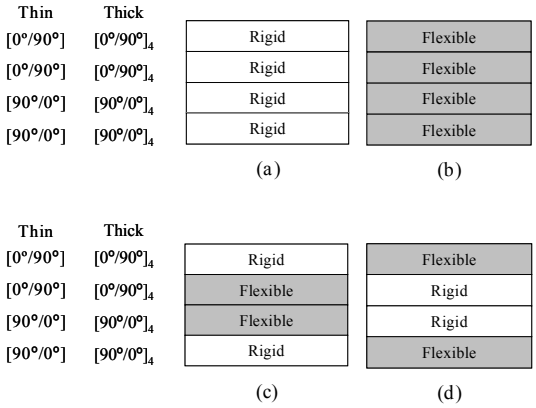

Figure 2: Stacking sequence of matrix hybrid composites (a) R, (b) F, (c) RFR and (d) FRF.

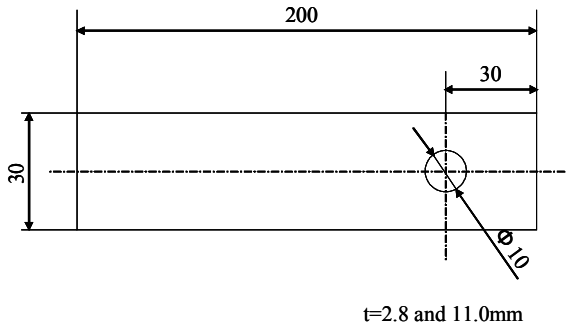

t=2.8 and 11.0mm

Figure 3: Geometry of specimen.

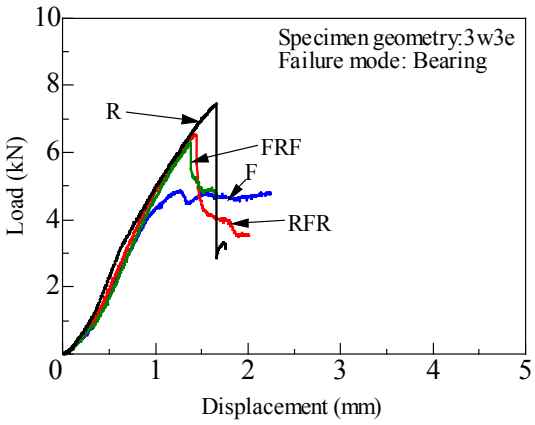

(a)

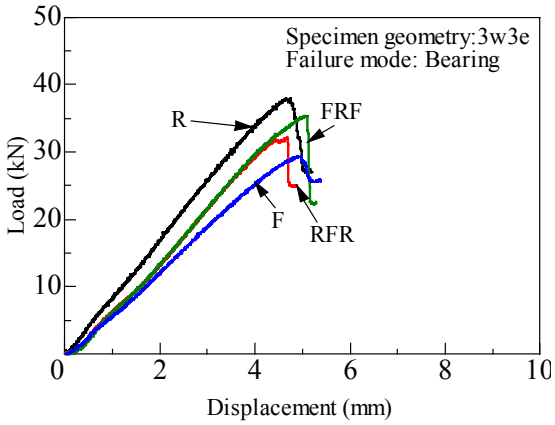

(b)

Figure 4: Load-displacement curves of (a) thin specimen (b) thick specimen

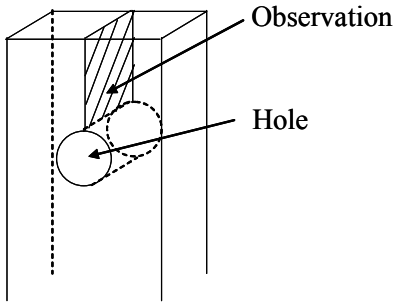

Figure 5: Observation part of specimen after joint test.

Table II: Experimental results of joint test.

	Thickness, t (mm)	Maximum load, P (kN)	P/P_R (%)	P/t (kN/mm)
R (thin)	2.8	7.44	100.0	2.66
F (thin)		4.84	65.1	1.73
RFR (thin)		6.53	87.8	2.33
FRF (thin)		6.30	84.7	2.25
R (thick)	11.0	37.80	100.0	3.44
F (thick)		29.20	77.2	2.65
RFR (thick)		32.00	84.7	2.91
FRF (thick)		35.30	93.4	3.21

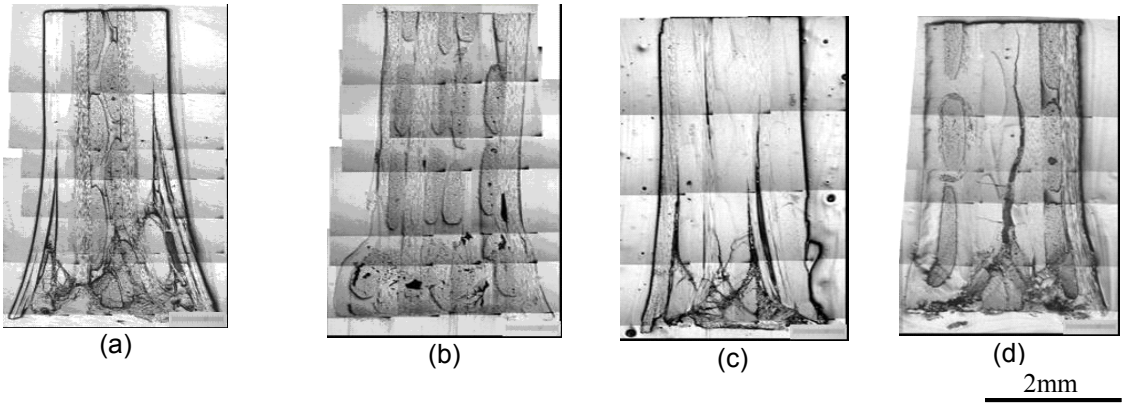

Figure 6: Fracture aspects of thin specimen in (a) R, (b) F, (c) RFR and (d) FRF

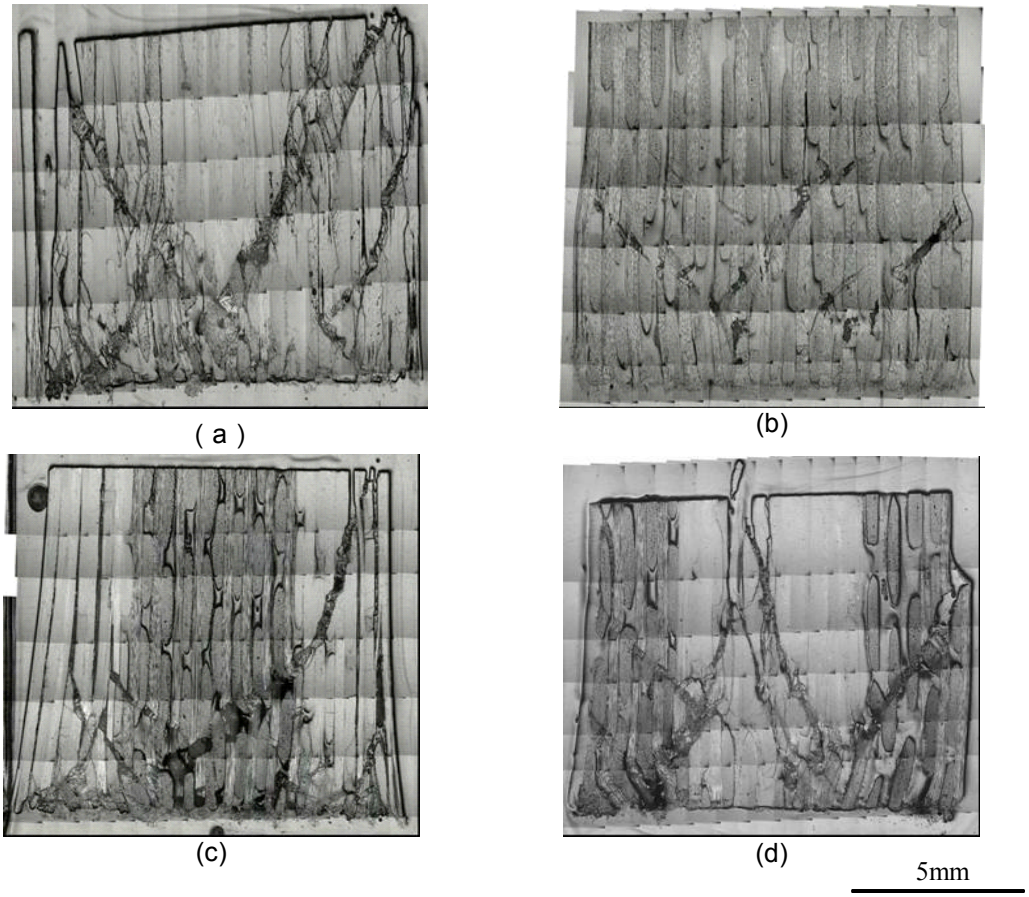

Figure 7: Fracture aspects of thick specimen in (a) R, (b) F, (c) RFR and (d) FRF